

# Temperature-Dependent Reversal of Phase Segregation in Mixed-Halide Perovskites

Adam D. Wright, Jay. B. Patel, Michael B. Johnston, and Laura M. Herz\*

Understanding the mechanism of light-induced halide segregation in mixed-halide perovskites is essential for their application in multijunction solar cells. Here, photoluminescence spectroscopy is used to uncover how both increases in temperature and light intensity can counteract the halide segregation process. It is observed that, with increasing temperature, halide segregation in  $\text{CH}_3\text{NH}_3\text{Pb}(\text{Br}_{0.4}\text{I}_{0.6})_3$  first accelerates toward  $\approx 290$  K, before slowing down again toward higher temperatures. Such reversal is attributed to the trade-off between the temperature activation of segregation, for example through enhanced ionic migration, and its inhibition by entropic factors. High light intensities meanwhile can also reverse halide segregation; however, this is found to be only a transient process that abates on the time scale of minutes. Overall, these observations pave the way for a more complete model of halide segregation and aid the development of highly efficient and stable perovskite multijunction and concentrator photovoltaics.

solar cells.<sup>[15]</sup> Tandem perovskite–perovskite<sup>[16–18]</sup> and perovskite–silicon<sup>[19–21]</sup> solar cells are especially promising commercially,<sup>[15,22,23]</sup> having already demonstrated PCEs exceeding those of single-junction silicon solar cells.<sup>[4,5]</sup> Incipient studies have further suggested potential for applications in solar concentrator cells that enable PCEs above the standard Shockley–Queisser limit.<sup>[24–26]</sup>

Successful implementation of perovskites in the top cells of tandem perovskite photovoltaic devices has however been hampered by the phenomenon of halide segregation,<sup>[27–29]</sup> which afflicts the mixed iodide–bromide compositions used to achieve the wide-bandgap ( $>1.7$  eV<sup>[22,23]</sup>) perovskites desired for sun-facing layers harvesting the high-energy parts of the solar spectrum. Under above-bandgap

illumination<sup>[27]</sup> or charge-carrier injection,<sup>[30–32]</sup> these materials undergo a demixing process, resulting in the formation of localized regions of iodide-rich and bromide-rich phases.<sup>[33–36]</sup> Removal of the external stimulus results in recovery from the segregation.<sup>[27,37–39]</sup> Although this reversible phase separation only affects a small minority of the perovskite volume,<sup>[34,40]</sup> the resultant spatially inhomogeneous bandgap seriously undermines the suitability of mixed-halide perovskites for tandem cell applications, not only by limiting the bandgap tunability necessary for such devices<sup>[41]</sup> but also through adversely affecting charge-carrier extraction<sup>[41–43]</sup> and recombination,<sup>[44]</sup> and causing voltage losses.<sup>[40,45]</sup> Consequently, considerable research attention has been devoted to understanding this phenomenon in order to prevent it, as laid out in several recent review articles.<sup>[46–50]</sup>

The precise mechanism of light-induced halide segregation remains contentious, with the proposed microscopic models falling into three broad categories.<sup>[47,48,51,52]</sup> The first set of models identify localized lattice strain as the driving force for halide segregation. This strain either arises from intrinsic lattice mismatch between the iodide and bromide ions<sup>[53]</sup> or is caused by the formation of polarons, that is, photoexcited charge carriers and their associated lattice distortion.<sup>[54–60]</sup> The second set of models (“bandgap-difference” models) meanwhile suggest the free energy reduction achieved by photoexcited charge carriers when funneling into spontaneously formed low-bandgap iodide-rich domains as the cause of halide segregation.<sup>[29,52,61–65]</sup> The third set of models invoke photogenerated charge-carrier gradients<sup>[66]</sup> or local electric fields<sup>[39,41,67,68]</sup> resulting in defect-mediated halide ion migration. This set of models requires

## 1. Introduction

Metal halide perovskites perform particularly well as photovoltaic active layers,<sup>[1–3]</sup> with the record power conversion efficiency (PCE) of single-junction perovskite solar cells now in excess of 25% after just over a decade of development.<sup>[4,5]</sup> This success derives from excellent optoelectronic properties combined with facile and inexpensive fabrication routes.<sup>[6,7]</sup> Straightforward variation of their chemical composition ( $\text{ABX}_3$ , A = methylammonium(MA)/formamidinium(FA)/Cs, B = Pb/Sn, X = I/Br/Cl) results in bandgap tuning across a wide spectral range of around 1.2 to 2.3 eV,<sup>[8–11]</sup> enabling versatile application in light-emitting diodes,<sup>[12]</sup> lasers,<sup>[13,14]</sup> and multijunction

A. D. Wright, J. B. Patel, M. B. Johnston, L. M. Herz  
Clarendon Laboratory, Department of Physics  
University of Oxford  
Parks Road, Oxford OX1 3PU, UK  
E-mail: laura.herz@physics.ox.ac.uk

L. M. Herz  
Institute for Advanced Study  
Technical University of Munich (TUM)  
Lichtenbergstraße 2a, 85748 Garching bei München, Germany

 The ORCID identification number(s) for the author(s) of this article can be found under <https://doi.org/10.1002/adma.202210834>.

© 2023 The Authors. Advanced Materials published by Wiley-VCH GmbH. This is an open access article under the terms of the Creative Commons Attribution License, which permits use, distribution and reproduction in any medium, provided the original work is properly cited.

DOI: 10.1002/adma.202210834

differential halide mobilities, and so is related to recently proposed mechanisms in which trapped holes preferentially oxidize iodide ions to more mobile species.<sup>[69–71]</sup> Despite the multiplicity of models, to date none have been able to fully explain all reported observations of light-induced halide segregation.<sup>[47,70,72]</sup>

Understanding the influence of temperature and light intensity on halide segregation is of particular interest for the real-world application and commercialization of perovskite tandem solar cells. Whereas in many research laboratories, photovoltaic devices are typically tested under an illumination intensity of 100 mW cm<sup>-2</sup> (corresponding to 1 sun, AM1.5) at 25 °C, cell temperature outdoors can reach 60 °C<sup>[73]</sup> while concentrator solar cells may experience up to 200 W cm<sup>-2</sup>.<sup>[24,26]</sup> Despite the evident importance of temperature and light intensity on performance, the field still lacks a clear picture of their effect on halide segregation. Photo-segregation kinetics in the temperature range 150–375 K have been suggested to be governed by an Arrhenius relation,<sup>[27,52,63,66,74,75]</sup> whose activation energy has been associated with that of halide ion migration.<sup>[27,63,66,76,77]</sup> Such effects may be expected because higher temperatures may hasten ionic motion. However, increased temperature should also enhance the entropic contribution to the free energy of a thermodynamic system, and so promote the remixing of the I-rich and Br-rich phases.<sup>[46]</sup> Recovery from halide segregation in the dark has been attributed to entropy of mixing,<sup>[53,54,61]</sup> and has been measured to speed up with increasing temperature (also with an Arrhenius relationship);<sup>[63]</sup> however, the entropic effect on the segregation dynamics is still surprisingly unclear at this point. The conflicting contributions of temperature to halide segregation are mirrored by those of light intensity. Higher excitation power has been widely reported to speed up segregation,<sup>[33,39,54,56,61–63]</sup> above some illumination threshold<sup>[61–64]</sup> which increases with temperature due to entropic effects.<sup>[63]</sup> Remarkably however, sufficiently high excitation powers have sometimes been shown to reverse segregation, either entirely<sup>[59,60]</sup> or partially.<sup>[78–80]</sup> Clearly, further investigation into the role of temperature and light intensity in halide segregation is needed<sup>[46,47]</sup> in order to establish a more unified picture, given its direct relevance to the performance of mixed-halide perovskite tandem and concentrator solar cells under operating conditions.

In this work, we investigate the influence of temperature and light intensity on light-induced halide segregation in MAPb(Br<sub>0.4</sub>I<sub>0.6</sub>)<sub>3</sub> by measuring changes in the photoluminescence (PL) spectra across an exceptionally wide parameter space. We reveal a reversal in the temperature trend in halide segregation rate, which speeds up as temperature is increased from 125 K to ≈290 K, but slows down again with further increases in temperature. This trend holds across a wide range of excitation intensities, and clearly demonstrates the opposing influences of kinetic and entropic factors on halide segregation. We further show that while halide remixing indeed occurs at highly elevated light intensities, and becomes more pronounced at higher temperatures, this effect is only transient, reversing on its own over the time scale of minutes under continued illumination. We utilize our findings to elucidate the validity of the most commonly examined models describing the origins of halide segregation, and discuss their relevance to applications of mixed-halide perovskites in tandem and concentrator solar cells.

## 2. Results

### 2.1. Temperature and Light-Intensity Dependence of Halide Segregation

The progress of halide segregation under photoexcitation may be tracked via measurement of the absorption,<sup>[33,61–63,76,81]</sup> X-ray diffraction (XRD),<sup>[61,65,82–85]</sup> or PL<sup>[27,39,41,54,61,62,65,66,76,86,87]</sup> spectra. Whereas light absorption and XRD measurements probe the volume average of the mixed-halide perovskite, the PL spectra are dominated by emission from the low-bandgap iodide-rich domains, into which charge carriers funnel.<sup>[29,61,82]</sup> PL measurements therefore have the advantage of being highly sensitive to halide segregation,<sup>[29,78]</sup> in which fractions of the material ranging from ≈20%<sup>[27,33]</sup> to as little as ≈1%<sup>[27,30]</sup> have been estimated to participate. In contrast, the absorption spectrum, especially above the bandgap, is usually barely affected by halide segregation.<sup>[41,61,81]</sup> The archetypal mixed-halide perovskite series MAPb(Br<sub>x</sub>I<sub>1-x</sub>)<sub>3</sub> has been studied extensively<sup>[46,47]</sup> and segregates for halide ratios 0.2 < x < 1.<sup>[27,56,66]</sup> While the x = 0.5 composition has been widely investigated in halide-segregation studies,<sup>[39,41,61,63,82]</sup> mixed halides with x = 0.4 result in a bandgap that is optimal for top cells<sup>[88]</sup> in perovskite-silicon tandems.<sup>[18,30,82,85,88]</sup> Mixed-halide perovskites with lower bromide fractions exhibit slower segregation rates,<sup>[27,65]</sup> aiding the temporal resolution of changes that occur under illumination, while the correlation between their degree of phase segregation and PL intensity is stronger.<sup>[65]</sup> Here, we study both MAPb(Br<sub>0.4</sub>I<sub>0.6</sub>)<sub>3</sub> and MAPb(Br<sub>0.5</sub>I<sub>0.5</sub>)<sub>3</sub> solution-processed thin films, topped with a layer of poly(methyl methacrylate) (PMMA) to exclude atmospheric influence on halide segregation dynamics,<sup>[39]</sup> prepared as described in the Supporting Information.

To explore the temperature-dependent nature of the halide segregation process, we measured the evolution of the PL spectra of PMMA-coated MAPb(Br<sub>0.4</sub>I<sub>0.6</sub>)<sub>3</sub> films under illumination at temperatures between 125 and 375 K. Experiments were conducted on fresh thin-film regions for each new measurement and only those runs were analyzed for which permanent material degradation could be excluded. **Figure 1** shows the time dependence of the normalized PL spectra recorded at 200, 295, and 325 K under 5 W cm<sup>-2</sup> excitation with 532 nm light. At 295 K, the emission initially peaks at 1.79 eV before redshifting within seconds and settling around 1.64 eV, consistent with previous reports for this material.<sup>[27,78,89,90]</sup> These dynamics capture the initial emission from predominantly mixed-halide domains, followed by growth in emission from iodide-rich domains at lower emission energy, typically corresponding to a material with bromide content x ≈ 0.2.<sup>[27,47,61,62,84,91]</sup> We note that the energy of the initial mixed-phase emission blueshifts with increasing temperature, as is characteristic for the bandgap shifts of lead halide perovskites,<sup>[92]</sup> while the iodide-rich peak shows the same trend,<sup>[52]</sup> which Vicente et al.<sup>[80]</sup> attributed to entropically driven re-homogenization of bromide into the iodide-rich regions. The shift in the PL peak at 325 K appears to proceed via emission at intermediate energy, similar to that observed by Mao et al.<sup>[93]</sup> and reminiscent of other previously reported transient emissions.<sup>[68,78,80,94]</sup>

These false-color plots of normalized PL spectra show an easily identifiable “switch-over” point where the intensities

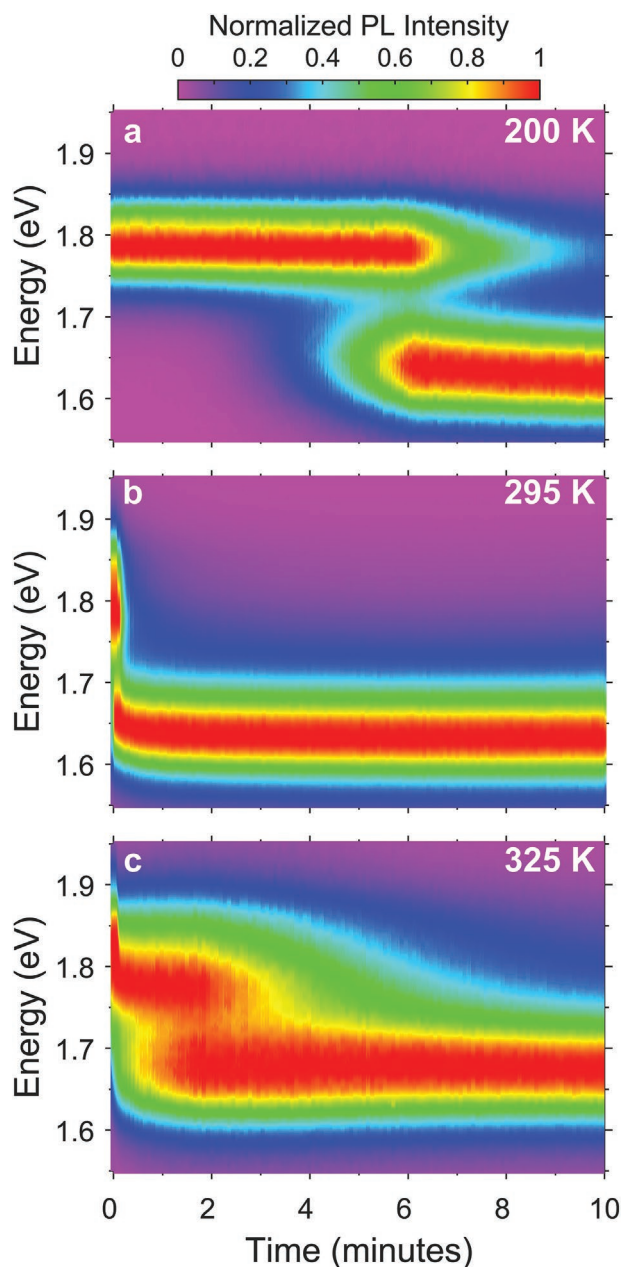


**Figure 1.** a–c) Normalized time-dependent PL spectra of MAPb(Br<sub>0.4</sub>I<sub>0.6</sub>)<sub>3</sub> thin films under 5 W cm<sup>-2</sup> excitation at 532 nm at temperatures of 200 K (a), 295 K (b), and 325 K (c). The individual PL spectra were normalized against their own maximum intensity within the range 1.51–1.98 eV.

from mixed-halide and iodide-rich phases momentarily become equal. Visual inspection of the normalized PL spectra shown in Figure 1 thus immediately reveals the temperature-dependent reversal of halide segregation rates. Halide segregation proceeds very slowly at 200 K which exhibits a long initial induction time up to the switch-over point, then accelerates rapidly as temperatures are raised to 295 K, but subsequently slows again as temperatures are raised further to 325 K. This reversal in trend is notable as halide segregation has typically been characterized as a simple Arrhenius process, for MAPb(Br<sub>0.4</sub>I<sub>0.6</sub>)<sub>3</sub> thin films<sup>[27,66]</sup> and other mixed-halide compositions.<sup>[63,75]</sup> We

note that although a threshold excitation intensity has been found to be required to induce halide segregation, and this increases with temperature, it lies well below our illumination conditions, only reaching 100 μW cm<sup>-2</sup> even at 363 K,<sup>[63]</sup> meaning that such threshold effects cannot explain the effects we observe. While there have been isolated reports of higher temperatures preventing halide segregation altogether,<sup>[46,56,57]</sup> the dynamic reversal in halide segregation kinetics as a function of temperature has not previously been reported.

In order to quantitatively capture such temperature-dependent reversal of halide segregation, it is necessary to identify a parameter describing the rate of halide segregation. The commonly used exponential fits to the growth of the iodide-rich PL feature<sup>[61,63,66,74]</sup> are unable to capture the latency that is evident in the halide segregation in Figure 1a and which is a common feature of processes involving nucleation.<sup>[54,64,65]</sup> Although more phenomenological expressions have been previously employed to capture this lag time in the process,<sup>[39,95]</sup> here we simply parametrize the halide segregation speed by the easily apparent “switch-over” time taken for the iodide-rich emission, as described above and detailed in the Supporting Information. This switch-over time,  $t_{sw}$ , is plotted in Figure 2a for MAPb(Br<sub>0.4</sub>I<sub>0.6</sub>)<sub>3</sub> between 125 and 375 K and under light intensities ranging from 10 mW cm<sup>-2</sup> to 300 W cm<sup>-2</sup>. It is evident that the reversal of trend shown in Figure 1 under 5 W cm<sup>-2</sup> also occurs under higher and lower light intensities, with halide segregation occurring most quickly at temperatures in the range of ≈275–300 K. Similarly, temperature-dependent measurements of the switch-over time for MAPb(Br<sub>0.5</sub>I<sub>0.5</sub>)<sub>3</sub> (bromide content  $x = 0.5$ ) are shown in Figure S1, Supporting Information, for light intensities from 30 mW cm<sup>-2</sup> to 40 W cm<sup>-2</sup>. A reversal of temperature-dependent trend in the switch-over time also occurs between 275 and 300 K, although compared to the case of  $x = 0.4$  it is somewhat less pronounced owing to the absence of higher-temperature data and moreover only is apparent under light intensities of 20 W cm<sup>-2</sup> and above.

Consistent with previous reports,<sup>[33,39,54,61,62,66,76,81]</sup> we generally observe halide segregation to proceed faster under higher light intensities. Figure 2b shows the evolution of the average emitted photon energy at 250 K, which exhibits the sigmoidal shape indicative of a lag time during the nucleation of iodide-rich domains<sup>[39,58,65]</sup> followed by segregation and ultimately saturation.<sup>[39,47,54,61,62,66]</sup> Interestingly, above room temperature however, segregation is not the fastest under the highest-intensity illumination (see Figure 2a, indicating that above 300 K switch-over times are shorter for intensities lower than 300 W cm<sup>-2</sup>). This observation is suggestive of the photothermal remixing proposed by Vicente et al.<sup>[79,80]</sup> in which higher incident intensities cause heating which drives entropic remixing of the halide ions, although such a mechanism might also be expected to result in the trend in halide segregation rate reversing at lower nominal temperatures for higher light intensities, which we do not observe. At low temperatures and light intensities, halide segregation was so slow that  $t_{sw}$  was longer than the duration of the measurement. Indeed, our observation of halide segregation at 150 K under 300 W cm<sup>-2</sup> is in line with the lowest-temperature reports of this phenomenon.<sup>[57,66]</sup>

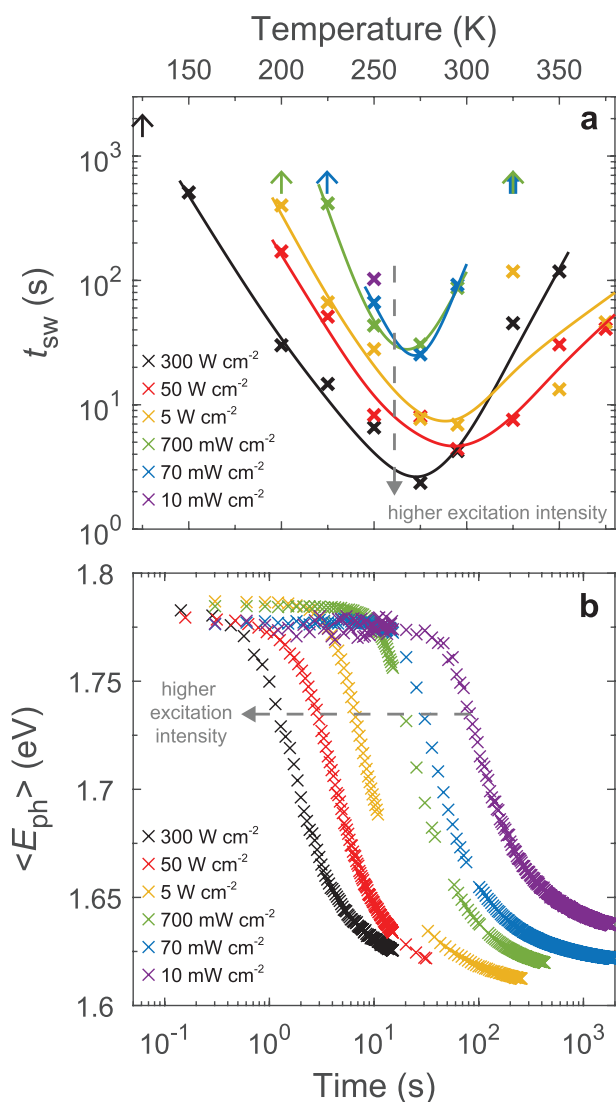


**Figure 2.** a) Temperature dependence of the switch-over time,  $t_{sw}$  for  $\text{MAPb}(\text{Br}_{0.4}\text{I}_{0.6})_3$  under light intensities ranging from  $10 \text{ mW cm}^{-2}$  to  $300 \text{ W cm}^{-2}$ .  $t_{sw}$  is the time taken for the PL intensity of the iodide-rich peak to exceed that of the mixed-halide peak. The solid lines are guides to the eye, indicating that maximum halide segregation rates (minimum  $t_{sw}$ ) are reached at temperatures of  $\approx 275\text{--}300 \text{ K}$ . The upward arrows indicate the duration of experiments for which halide segregation was so slow that the switch-over condition was not achieved and thus represent a lower bound on the  $t_{sw}$  under these conditions. b) Time dependence of the average photon energy  $\langle E_{ph} \rangle$  of the PL emission at  $250 \text{ K}$  is shown under excitation intensities ranging from  $10 \text{ mW cm}^{-2}$  to  $300 \text{ W cm}^{-2}$ .

## 2.2. Light-Induced Remixing

Highly elevated light intensities have also recently been reported to inhibit halide segregation, which we examine here in detail. For example, several studies have observed that following halide segregation in thin films of  $\text{MAPb}(\text{Br}_x\text{I}_{1-x})_3$  with  $0.33 \leq x \leq 0.9$  the final PL emission gradually blueshifts with time, with the shift becoming more pronounced as the light intensity is raised from  $10 \text{ mW cm}^{-2}$  to  $16 \text{ W cm}^{-2}$ .<sup>[78–80]</sup> This blueshift has been attributed to local photothermal remixing<sup>[79,80]</sup> following the

rapid formation of especially iodide-rich domains, and does not recover the initial pristine mixed-halide composition, that is, represents only partial reversal of halide segregation. However, one much more dramatic report has been made by Mao et al.<sup>[59]</sup> of almost total recovery from halide segregation in single-crystal microplatelets of  $\text{MAPb}(\text{Br}_{0.8}\text{I}_{0.2})_3$  when the light intensity was increased from  $10$  to  $200 \text{ W cm}^{-2}$  under pulsed excitation by a  $400 \text{ nm}$  laser at  $295 \text{ K}$ , as reproduced in Figure S2b, Supporting Information. These authors have reported that following initial  $10 \text{ W cm}^{-2}$  excitation, the PL emission redshifts from  $2.25$  to  $1.75 \text{ eV}$  as expected for halide segregation, but upon application of the  $200 \text{ W cm}^{-2}$  light, the main PL emission blueshifts to  $2.23 \text{ eV}$ , very closely approaching the initial mixed-phase emission—an effect attributed to halide remixing. Once the light intensity is reduced back to  $10 \text{ W cm}^{-2}$  after  $20 \text{ s}$ , halide segregation resumes and the PL emission again redshifts. Mao et al. attributed this remixing to the elimination of the strain gradients driving halide segregation, owing to the high charge-carrier density causing the polarons in the material to overlap, allowing entropy-driven remixing to dominate.

We here aim to re-produce such effects for the  $\text{MAPb}(\text{Br}_{0.4}\text{I}_{0.6})_3$  thin films under investigation, and to probe the extent to which they last beyond the initial period of tens of seconds explored in the study by Mao et al. **Figure 3** shows our measurements of the time-dependent PL emission from  $\text{MAPb}(\text{Br}_{0.4}\text{I}_{0.6})_3$  thin films when exposed to low and high light intensities, with care taken that the region of the sample under illumination did not drift spatially. At all three temperatures, initial exposure to  $5 \text{ W cm}^{-2}$  light resulted solely in the expected PL redshift caused by halide segregation. Increasing the incident light intensity to  $50 \text{ W cm}^{-2}$  did not cause any significant change in the PL, nor were any changes observed upon a return to the lower  $5 \text{ W cm}^{-2}$ . However, increasing the light intensity to a much higher  $300 \text{ W cm}^{-2}$  from  $5 \text{ W cm}^{-2}$  did result in a blueshift in the PL, indicative of some halide re-mixing. At a temperature of  $295 \text{ K}$  this blueshift was not very pronounced in comparison to that observed by Mao et al.,<sup>[59]</sup> as highlighted in Figure S2, Supporting Information, in which the PL spectra from the two studies are presented alongside each other. We note that for the  $\text{MAPb}(\text{Br}_{0.4}\text{I}_{0.6})_3$  thin films we examined here, the observed blueshift occurred within  $1 \text{ s}$  of exposure to  $300 \text{ W cm}^{-2}$  intensity, while for the  $\text{MAPb}(\text{Br}_{0.8}\text{I}_{0.2})_3$  microplatelets examined by Mao et al.<sup>[59]</sup> a slower shift over  $\approx 20 \text{ s}$  occurred under  $200 \text{ W cm}^{-2}$  intensity, most likely because of higher bromide content and higher crystallinity for their materials.<sup>[9,46]</sup> However, we note that importantly, the remixing we observed here proves to be only transient, as the PL soon redshifted again under continued illumination with  $300 \text{ W cm}^{-2}$  light, indicating that the halides re-segregated again over the time scale of minutes. Furthermore, as shown in Figure S3, Supporting Information, when pristine, well-mixed films of  $\text{MAPb}(\text{Br}_{0.4}\text{I}_{0.6})_3$  are excited with  $300 \text{ W cm}^{-2}$  at the same temperatures, they respond by rapid halide segregation, showing that highly elevated intensities do not as such provide a stabilizing force against halide segregation. Interestingly, such halide segregation of a pristine film under  $300 \text{ W cm}^{-2}$  excitation (as shown in Figure S3, Supporting Information) proceeds on similar timescales to those of the re-segregation process observed in Figure 3 following the brief re-mixing effect. Increasing the

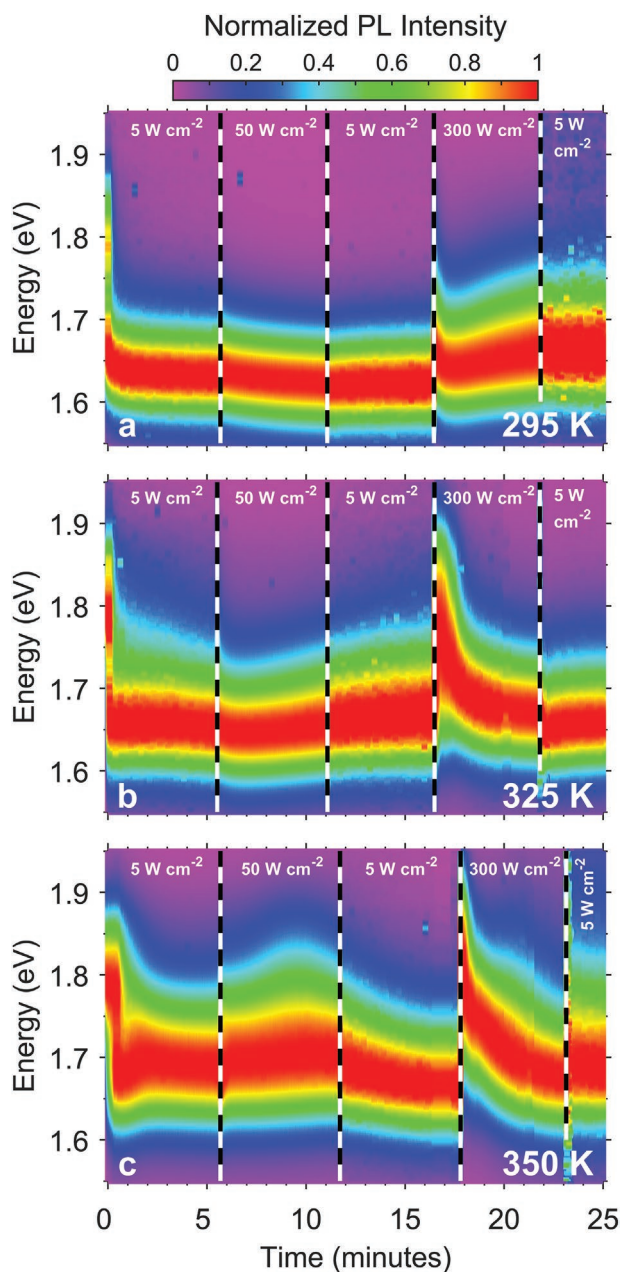


**Figure 3.** a–c) Evolution of normalized PL emission spectra from  $\text{MAPb}(\text{Br}_{0.4}\text{I}_{0.6})_3$  thin films at 295 K (a), 325 K (b), and 350 K (c) under successive continuous-wave excitation intensities of 5, 50, 5, 300, and  $5 \text{ W cm}^{-2}$  at 532 nm. These conditions correspond to approximate steady-state charge-carrier densities of  $2.4 \times 10^{15}$ ,  $1.6 \times 10^{16}$ ,  $2.4 \times 10^{15}$ ,  $5.2 \times 10^{16}$ , and  $2.4 \times 10^{15} \text{ cm}^{-3}$ , respectively (see Section S2.1, Supporting Information). The dashed black-and-white lines indicate the transitions between the different excitation intensities. The individual PL spectra were normalized against their own maximum intensity within the range 1.51–1.98 eV.

temperature enhances the effect of remixing (see Figure 3 and Figure S4, Supporting Information) likely because of the photothermal remixing effect proposed by Vicente et al.,<sup>[80]</sup> with the PL spectra recorded at 350 K even blueshifting past that recorded initially for the mixed-phase PL emission. Importantly,

in all cases the remixing effect is transient, only very briefly reversing apparent halide segregation, after which it re-commences with much the same speed as originally observed for the pristine, well-mixed material, for which such elevated intensities seem to have no stabilizing effect at all. We note that the transience and short timescale of this remixing distinguishes it from the light-induced defect formation that has been reported to promote protection from material degradation in metal halide perovskites over longer timescales.<sup>[65,96]</sup>

### 3. Discussion

Our findings have important implications for the identification of mechanisms underpinning halide segregation in lead iodide–bromide perovskites, and for their application in tandem and concentrator solar cells. We begin our discussion by examining how our findings can be rationalized by various models that have been proposed for the halide segregation phenomenon. We note that below room temperature, our observations are qualitatively consistent with the widely reported temperature-activated enhancement of the segregation rate,<sup>[27,52,63,66,74,75]</sup> although we did not find a good agreement with an Arrhenius relationship. However, at temperatures around 275–300 K for both  $\text{MAPb}(\text{Br}_{0.4}\text{I}_{0.6})_3$  and  $\text{MAPb}(\text{Br}_{0.5}\text{I}_{0.5})_3$ , we find a reversal of halide segregation dynamics, with slower rates for higher temperatures. We attribute this observed reversal to a trade-off between kinetic enhancement from increased halide ion mobilities and entropic hindrance of halide segregation with increasing temperature.

Theoretical backing for entropic hindrance of phase segregation can be found from calculated thermodynamics phase diagrams assuming presence of some strain,<sup>[53,54]</sup> and bandgap-difference,<sup>[64]</sup> which indicate that the initial mixed phase should be stabilized against segregation at sufficiently high temperature, in particular under strong photoexcitation. However, such phase diagrams also posit that the initial mixed phase should be thermodynamically unstable even in the dark below some critical temperature, variously calculated as 343,<sup>[53]</sup> 266,<sup>[64]</sup> and 190 K<sup>[54]</sup> for  $\text{MAPb}(\text{Br}_x\text{I}_{1-x})_3$ . While of course the thermodynamic favorability of a process does not necessarily determine its rate,<sup>[72]</sup> these predictions are nonetheless difficult to reconcile with the above-mentioned reports that halide segregation is temperature-activated at lower temperatures, and reports of efficient solid-state halide ion exchange between lead iodide and bromide films upon physical contact.<sup>[76]</sup>

Explanations for the phenomenon of light-induced remixing have been proposed either in terms of photothermal heating driving entropic remixing<sup>[79,80]</sup> or polaron overlap leading to the elimination of strain gradients.<sup>[59,60]</sup> Whereas bandgap-difference models fare better than polaron models at explaining the excitation threshold<sup>[47,64]</sup> necessary for halide segregation to take place at all, they struggle to rationalize such light-induced halide remixing since increasing light intensity is expected to strictly drive segregation more strongly.<sup>[51,64]</sup> However, the polaronic conception of remixing proposed by Mao et al.,<sup>[59]</sup> which assumes that at sufficiently high intensities, interpenetration of polarons leads to elimination of lattice-strain and therefore halide segregation, cannot explain why this effect would

be transient, as we show here, even when light intensities are kept high. The occurrence of the transient light-induced halide remixing we observe here for MAPb(Br<sub>0.4</sub>I<sub>0.6</sub>)<sub>3</sub> thus demands an alternate explanation. We further note that the dynamics of the re-segregation process following the remixing upon the sudden increase in excitation power are very similar to those of the initial segregation dynamics observed for a pristine film. These findings suggest that the initial flood of photoexcited charge carriers following the increase in intensity only momentarily resets the situation in the material, after which the previous equilibrium of segregated material quickly re-establishes itself.

We propose that this reset is a photothermal effect, triggered by the sudden arrival of an abundance of excited charge carriers generated by the newly applied, highly elevated illumination intensity. This flood of charge carriers funnels into the relatively small volume of iodide-rich domains formed under the previous, lower excitation power, with their size and abundance having been determined by the opposing forces of entropic remixing and light-induced halide segregation at the previous, lower light intensity. Given that such charge-carrier funneling has been shown to occur on the picosecond time scale in slightly segregated materials,<sup>[44]</sup> while ionic rearrangements take minutes to occur, the system is therefore momentarily imbalanced. Importantly, upon arrival at the iodide-rich inclusions, each charge-carrier pair loses a quantum of energy corresponding to the bandgap difference between the mixed phase and iodide-rich phase ( $\approx 175$  meV). Owing to the low thermal conductivity of metal halide perovskites,<sup>[97]</sup> the energy dissipated by the charge carriers results in local heating of the iodide-rich domains. The sudden strong increase in illumination intensity therefore results in a significant increase in the heat dumped into the existing small volume of iodide-rich domains, elevating their temperature substantially. As we showed in Figure 2, for MAPb(Br<sub>0.4</sub>I<sub>0.6</sub>)<sub>3</sub> at temperatures above  $\approx 290$  K a sufficient increase in temperature will result in the balance tipping in favor of entropic remixing, thus explaining the observed reversal of halide segregation.

This picture also explains why such remixing is however transient under prolonged high illumination intensities. Under such conditions, mixed-halide material will continue to segregate, generating iodide-rich domains as a larger volume fraction, which will gradually distribute the heat load arising from charge-carrier funneling more evenly across the film. As a result, the temperature within the iodide-rich domains eventually falls below that needed for entropic effects to dominate and halide segregation again re-emerges. Therefore, the transience of the remixing observed in Figure 3 is a consequence of the timescale of iodide-rich domain growth (for which the switch-over time,  $t_{sw}$ , shown in Figure 2a is a proxy) being too slow to counterbalance the entropic remixing induced by charge-carrier funneling and photothermal heating under higher excitation intensities.<sup>[79,80]</sup> This model also explains why direct excitation of a pristine, fully mixed iodide–bromide perovskite with high illumination intensity still induces halide segregation (Figure S3d–f, Supporting Information): since such a material does not initially contain iodide-rich domains, the imbalance between locally intensified heating and segregating forces is never present in the first place and the material simply segregates rapidly. We further note that this explanation is in accordance with our observation of more pronounced light-induced

remixing at higher temperatures (Figure 3). Since the switch-over time  $t_{sw}$  displays a parabolic temperature-dependence (Figure 2a) with a minimum near  $\approx 290$  K, any remixing effects are expected to increase prominently with temperature increases above that point, as we indeed observe in Figure 3.

From an application perspective, our observation of temperature-dependent reversal of halide segregation and the transient nature of halide remixing under high illumination intensities has important implications for tandem photovoltaics and concentrator cells. Clearly, it is somewhat unfortunate that the perovskite compositions with the most suitable bandgap energies for tandem cells with silicon exhibit the fastest halide segregation rates near room temperature. However, the ensuing reversal of halide segregation speeds toward elevated temperatures means that, provided materials are optimized to be stable at room temperature, more elevated cell operating temperatures outdoors in excess of  $60$  °C<sup>[73]</sup> will not pose a problem. Even higher temperatures reached under solar concentrator scenarios would be beneficial toward reducing halide segregation, as these iodide–bromide perovskites would clearly be in the entropic limit of the curve. However, as we show, halide remixing deriving from high light intensities alone may not necessarily be beneficial to concentrator cell operation as the effect appears to be relatively short-lived.

## 4. Conclusion

We have systematically demonstrated how changes in temperature and light intensity affect halide segregation in lead bromide–iodide perovskite thin films with intermediate bromide content. We find a reversal in the halide segregation rate around room temperature, resulting from a trade-off between the countervailing influences of entropic remixing and temperature-activated halide ion migration. We further show that while an apparent light-induced halide remixing effect occurs in MAPb(Br<sub>0.4</sub>I<sub>0.6</sub>)<sub>3</sub> under high illumination intensities of  $300$  W cm<sup>-2</sup>, such effects are shortlived, and arise from charge-carrier funneling resulting in photothermal heating and entropic remixing of the iodide-rich domains, after which halide segregation re-forms larger iodide-rich domains of sufficient size that spread the heat load, thus re-establishing the segregation dynamic. Such understanding of the influences of temperature and light intensity on halide segregation provides critical insight into the mechanisms causing such effects, and a grasp on how it impacts the application of mixed-halide perovskites in multijunction and concentrator solar cells.

## Supporting Information

Supporting Information is available from the Wiley Online Library or from the author.

## Acknowledgements

The authors thank the Engineering and Physical Sciences Research Council (EPSRC), UK, for financial support. L.M.H. thanks the Institute for Advanced Study at the Technical University of Munich for support through a Hans Fischer Senior Fellowship.

## Conflict of Interest

The authors declare no conflict of interest.

## Data Availability Statement

The data that support the findings of this study are available from the corresponding author upon reasonable request.

## Keywords

halide segregation, mixed-halide perovskites, photoluminescence, photovoltaic devices, thin films

Received: November 21, 2022

Revised: January 24, 2023

Published online: March 24, 2023

- [1] A. Kumar Jena, A. Kulkarni, T. Miyasaka, *Chem. Rev.* **2019**, *119*, 3036.
- [2] A. Kojima, K. Teshima, Y. Shirai, T. Miyasaka, *J. Am. Chem. Soc.* **2009**, *131*, 6050.
- [3] M. M. Lee, J. Teuscher, T. Miyasaka, T. N. Murakami, H. J. Snaith, *Science* **2012**, *338*, 643.
- [4] M. A. Green, E. D. Dunlop, J. Hohl-Ebinger, M. Yoshita, N. Kopidakis, K. Bothe, D. Hinken, M. Rauer, X. Hao, *Prog. Photovoltaics* **2022**, *30*, 687.
- [5] NREL, <https://www.nrel.gov/pv/cell-efficiency.html> (accessed: October 2022).
- [6] L. M. Herz, *ACS Energy Lett.* **2017**, *2*, 1539.
- [7] M. B. Johnston, L. M. Herz, *Acc. Chem. Res.* **2016**, *49*, 146.
- [8] J. Noh, S. Im, J. Heo, T. Mandal, S. Seok, *Nano Lett.* **2013**, *13*, 1764.
- [9] W. Rehman, D. P. McMeekin, J. B. Patel, R. L. Milot, M. B. Johnston, H. J. Snaith, L. M. Herz, *Energy Environ. Sci.* **2017**, *10*, 361.
- [10] K. J. Savill, A. M. Ulatowski, L. M. Herz, *ACS Energy Lett.* **2021**, *6*, 2413.
- [11] Y. Chen, S. G. Motti, R. D. J. Oliver, A. D. Wright, H. J. Snaith, M. B. Johnston, L. M. Herz, M. R. Filip, *J. Phys. Chem. Lett.* **2022**, *13*, 4184.
- [12] L. Protesescu, S. Yakunin, M. I. Bodnarchuk, F. Krieg, R. Caputo, C. H. Hendon, R. X. Yang, A. Walsh, M. V. Kovalenko, *Nano Lett.* **2015**, *15*, 3692.
- [13] G. Xing, N. Mathews, S. S. Lim, N. Yantara, X. Liu, D. Sabba, M. Grätzel, S. Mhaisalkar, T. C. Sum, *Nat. Mater.* **2014**, *13*, 476.
- [14] X. Yang, H. Qiu, S. Hu, C. Cao, Z. Xie, Q. Jiang, F. Huang, C. X. Sheng, *Mater. Lett.* **2022**, *313*, 131843.
- [15] T. C. J. Yang, P. Fiala, Q. Jeangros, C. Ballif, *Joule* **2018**, *2*, 1421.
- [16] G. E. Eperon, T. Leijtens, K. A. Bush, R. Prasanna, T. Green, J. T. W. Wang, D. P. McMeekin, G. Volonakis, R. L. Milot, R. May, A. Palmstrom, D. J. Slotcavage, R. A. Belisle, J. B. Patel, E. S. Parrott, R. J. Sutton, W. Ma, F. Moghadam, B. Conings, A. Babayigit, H. G. Boyen, S. Bent, F. Giustino, L. M. Herz, M. B. Johnston, M. D. McGehee, H. J. Snaith, *Science* **2016**, *354*, 861.
- [17] A. Rajagopal, Z. Yang, S. B. Jo, I. L. Braly, P. W. Liang, H. W. Hillhouse, A. K. Jen, *Adv. Mater.* **2017**, *29*, 1702140.
- [18] R. Lin, K. Xiao, Z. Qin, Q. Han, C. Zhang, M. Wei, M. I. Saidaminov, Y. Gao, J. Xu, M. Xiao, A. Li, J. Zhu, E. H. Sargent, H. Tan, *Nat. Energy* **2019**, *4*, 864.
- [19] K. A. Bush, A. F. Palmstrom, Z. J. Yu, M. Boccard, R. Cheacharoen, J. P. Mailoa, D. P. McMeekin, R. L. Hoyer, C. D. Bailie, T. Leijtens, I. M. Peters, M. C. Minichetti, N. Rolston, R. Prasanna, S. Sofia, D. Harwood, W. Ma, F. Moghadam, H. J. Snaith, T. Buonassisi, Z. C. Holman, S. F. Bent, M. D. McGehee, *Nat. Energy* **2017**, *2*, 17009.
- [20] T. Duong, Y. Wu, H. Shen, J. Peng, X. Fu, D. Jacobs, E.-C. Wang, T. C. Kho, K. C. Fong, M. Stocks, E. Franklin, A. Blakers, N. Zin, K. McIntosh, W. Li, Y.-B. Cheng, T. P. White, K. Weber, K. Catchpole, *Adv. Energy Mater.* **2017**, *7*, 1700228.
- [21] A. Al-Ashouri, E. Köhnen, B. Li, A. Magomedov, H. Hempel, P. Caprioglio, J. A. Márquez, A. B. M. Vilches, E. Kasparavicius, J. A. Smith, N. Phung, D. Menzel, M. Grischek, L. Kegelmann, D. Skroblin, C. Gollwitzer, T. Malinauskas, M. Jošt, G. Matič, B. Rech, R. Schlattmann, M. Topič, L. Korte, A. Abate, B. Stannowski, D. Neher, M. Stollerfoht, T. Unold, V. Getautis, S. Albrecht, *Science* **2020**, *370*, 1300.
- [22] A. W. Ho-Baillie, J. Zheng, M. A. Mahmud, F. J. Ma, D. R. McKenzie, M. A. Green, *Appl. Phys. Rev.* **2021**, *8*, 041307.
- [23] J. Werner, B. Niesen, C. Ballif, *Adv. Mater. Interfaces* **2018**, *5*, 1700731.
- [24] Q. Lin, Z. Wang, H. J. Snaith, M. B. Johnston, L. M. Herz, *Adv. Sci.* **2018**, *5*, 1700792.
- [25] Z. Wang, Q. Lin, B. Wenger, M. G. Christoforo, Y. H. Lin, M. T. Klug, M. B. Johnston, L. M. Herz, H. J. Snaith, *Nat. Energy* **2018**, *3*, 855.
- [26] P. Sadhukhan, A. Roy, P. Sengupta, S. Das, T. K. Mallick, M. K. Nazeeruddin, S. Sundaram, *Appl. Phys. Rev.* **2021**, *8*, 041324.
- [27] E. T. Hoke, D. J. Slotcavage, E. R. Dohner, A. R. Bowring, H. I. Karunadasa, M. D. McGehee, *Chem. Sci.* **2015**, *6*, 613.
- [28] D. J. Slotcavage, H. I. Karunadasa, M. D. McGehee, *ACS Energy Lett.* **2016**, *1*, 1199.
- [29] M. C. Brennan, S. Draguta, P. V. Kamat, M. Kuno, *ACS Energy Lett.* **2018**, *3*, 204.
- [30] I. L. Braly, R. J. Stoddard, A. Rajagopal, A. R. Uhl, J. K. Katahara, A. K. Jen, H. W. Hillhouse, *ACS Energy Lett.* **2017**, *2*, 1841.
- [31] T. Duong, H. K. Mulmudi, Y. Wu, X. Fu, H. Shen, J. Peng, N. Wu, H. T. Nguyen, D. Macdonald, M. Lockrey, T. P. White, K. Weber, K. Catchpole, *ACS Appl. Mater. Interfaces* **2017**, *9*, 26859.
- [32] Z. Xu, R. A. Kerner, J. J. Berry, B. P. Rand, *Adv. Funct. Mater.* **2022**, *32*, 2203432.
- [33] S. J. Yoon, S. Draguta, J. S. Manser, O. Sharia, W. F. Schneider, M. Kuno, P. V. Kamat, *ACS Energy Lett.* **2016**, *1*, 290.
- [34] A. Bernhardt, T. D. Ambagaspitiya, M. E. Kordes, K. L. A. Cimat, J. Chen, *ChemPhysChem* **2022**, *23*, 202200022.
- [35] X. Sun, Y. Zhang, W. Ge, *Light: Sci. Appl.* **2022**, *11*, 262.
- [36] H. Zhang, X. Fu, Y. Tang, H. Wang, C. Zhang, W. W. Yu, X. Wang, Y. Zhang, M. Xiao, *Nat. Commun.* **2019**, *10*, 1088.
- [37] M. Hu, C. Bi, Y. Yuan, Y. Bai, J. Huang, *Adv. Sci.* **2016**, *3*, 1500301.
- [38] G. Li, F. W. R. Rivarola, N. J. Davis, S. Bai, T. C. Jellicoe, F. De La Peña, S. Hou, C. Ducati, F. Gao, R. H. Friend, N. C. Greenham, Z. K. Tan, *Adv. Mater.* **2016**, *28*, 3528.
- [39] A. J. Knight, A. D. Wright, J. B. Patel, D. P. McMeekin, H. J. Snaith, M. B. Johnston, L. M. Herz, *ACS Energy Lett.* **2019**, *4*, 75.
- [40] S. Mahesh, J. M. Ball, R. D. Oliver, D. P. McMeekin, P. K. Nayak, M. B. Johnston, H. J. Snaith, *Energy Environ. Sci.* **2020**, *13*, 258.
- [41] A. J. Knight, J. B. Patel, H. J. Snaith, M. B. Johnston, L. M. Herz, *Adv. Energy Mater.* **2020**, *10*, 1903488.
- [42] K. Datta, B. T. van Gorkom, Z. Chen, M. J. Dyson, T. P. van der Pol, S. C. Meskers, S. Tao, P. A. Bobbert, M. M. Wienk, R. A. Janssen, *ACS Appl. Energy Mater.* **2021**, *4*, 6650.
- [43] Y. Guo, X. Yin, J. Liu, W. Que, *Matter* **2022**, *5*, 2015.
- [44] S. G. Motti, J. B. Patel, R. D. Oliver, H. J. Snaith, M. B. Johnston, L. M. Herz, *Nat. Commun.* **2021**, *12*, 6955.
- [45] W. Yang, H. Long, X. Sha, J. Sun, Y. Zhao, C. Guo, X. Peng, C. Shou, X. Yang, J. Sheng, Z. Yang, B. Yan, J. Ye, *Adv. Funct. Mater.* **2022**, *32*, 2110698.

- [46] A. J. Knight, L. M. Herz, *Energy Environ. Sci.* **2020**, *13*, 2024.
- [47] M. C. Brennan, A. Ruth, P. V. Kamat, M. Kuno, *Trends Chem.* **2020**, *2*, 282.
- [48] H. Choe, D. Jeon, S. J. Lee, J. Cho, *ACS Omega* **2021**, *6*, 24304.
- [49] Y. R. Wang, G. Yeong Kim, E. Kotomin, D. Moia, J. Maier, *J Phys Energy* **2022**, *4*, 011001.
- [50] R. R. Sumukam, P. Sahu, R. N. Savu, S. J. Khanam, Q. A. Alsulami, M. Banavoth, *Phys. Status Solidi RRL* **2022**, *16*, 2100576.
- [51] L. Tian, J. Xue, R. Wang, *Electronics* **2022**, *11*, 700.
- [52] I. M. Pavlovets, A. Ruth, I. Gushchina, L. Ngo, S. Zhang, Z. Zhang, M. Kuno, *ACS Energy Lett.* **2021**, *6*, 2064.
- [53] F. Brivio, C. Caetano, A. Walsh, *J. Phys. Chem. Lett.* **2016**, *7*, 1083.
- [54] C. G. Bischak, C. L. Hetherington, H. Wu, S. Aloni, D. F. Ogletree, D. T. Limmer, N. S. Ginsberg, *Nano Lett.* **2017**, *17*, 1028.
- [55] C. G. Bischak, A. B. Wong, E. Lin, D. T. Limmer, P. Yang, N. S. Ginsberg, *J. Phys. Chem. Lett.* **2018**, *9*, 3998.
- [56] P. Nandi, C. Giri, D. Swain, U. Manju, S. D. B. Mahanti, D. Topwal, *ACS Appl. Energy Mater.* **2018**, *1*, 3807.
- [57] X. Wang, Y. Ling, X. Lian, Y. Xin, K. B. Dhungana, F. Perez-Orive, J. Knox, Z. Chen, Y. Zhou, D. Beery, K. Hanson, J. Shi, S. Lin, H. Gao, *Nat. Commun.* **2019**, *10*, 695.
- [58] D. T. Limmer, N. S. Ginsberg, *J. Chem. Phys.* **2020**, *152*, 230901.
- [59] W. Mao, C. R. Hall, S. Bernardi, Y.-B. Cheng, A. Widmer-Cooper, T. A. Smith, U. Bach, *Nat. Mater.* **2021**, *20*, 55.
- [60] Y. Guo, X. Yin, D. Liu, J. Liu, C. Zhang, H. Xie, Y. Yang, W. Que, *ACS Energy Lett.* **2021**, *6*, 2502.
- [61] S. Draguta, O. Sharia, S. J. Yoon, M. C. Brennan, Y. V. Morozov, J. M. Manser, P. V. Kamat, W. F. Schneider, M. Kuno, *Nat. Commun.* **2017**, *8*, 200.
- [62] A. Ruth, M. C. Brennan, S. Draguta, Y. V. Morozov, M. Zhukovskiy, B. Janko, P. Zapol, M. Kuno, *ACS Energy Lett.* **2018**, *3*, 2321.
- [63] T. Elmelund, B. Seger, M. K. Kuno, P. V. Kamat, *ACS Energy Lett.* **2020**, *5*, 56.
- [64] Z. Chen, G. Brocks, S. Tao, P. A. Bobbert, *Nat. Commun.* **2021**, *12*, 2687.
- [65] K. Suchan, J. Just, P. Beblo, C. Reherman, A. Merdasa, R. Mainz, I. G. Schleblykin, E. Unger, *Adv. Funct. Mater.* **2022**, *33*, 2206047.
- [66] A. J. Barker, A. Sadhanala, F. Deschler, M. Gandini, S. P. Senanayak, P. M. Pearce, E. Mosconi, A. J. Pearson, Y. Wu, A. R. Srimath Kandada, T. Leijtens, F. De Angelis, S. E. Dutton, A. Petrozza, R. H. Friend, *ACS Energy Lett.* **2017**, *2*, 1416.
- [67] R. A. Belisle, K. A. Bush, L. Bertoluzzi, A. Gold-Parker, M. F. Toney, M. D. McGehee, *ACS Energy Lett.* **2018**, *3*, 2694.
- [68] X. Yang, C. Cao, S. Hu, H. Qiu, J. Ge, Q. Jiang, C. Sheng, *Vacuum* **2021**, *194*, 110624.
- [69] G. F. Samu, Á. Balog, F. De Angelis, D. Meggiolaro, P. V. Kamat, C. Janáky, *J. Am. Chem. Soc.* **2019**, *141*, 10812.
- [70] R. A. Kerner, Z. Xu, B. W. Larson, B. P. Rand, *Joule* **2021**, *5*, 2273.
- [71] J. T. Dubose, P. V. Kamat, *Acc. Mater. Res.* **2022**, *3*, 761.
- [72] T. L. Leung, Z. Ren, A. A. Syed, L. Grisanti, A. B. Djuris, J. Popovic, *ACS Energy Lett.* **2022**, *7*, 3500.
- [73] M. Jošt, B. Lipovšek, B. Glažar, A. Al-Ashouri, K. Brecl, G. Matič, A. Magomedov, V. Getautis, M. Topič, S. Albrecht, *Adv. Energy Mater.* **2020**, *10*, 2000454.
- [74] J. Cho, P. V. Kamat, *Adv. Opt. Mater.* **2021**, *9*, 2001440.
- [75] P. Nandi, Z. Li, Y. Kim, T. K. Ahn, N.-G. Park, H. Shin, *ACS Energy Lett.* **2021**, *6*, 837.
- [76] T. Elmelund, R. A. Scheidt, B. Seger, P. V. Kamat, *ACS Energy Lett.* **2019**, *4*, 1961.
- [77] L. McGovern, G. Grimaldi, M. H. Futscher, E. M. Hutter, L. A. Muscarella, M. C. Schmidt, B. Ehrler, *ACS Appl. Energy Mater.* **2021**, *4*, 13431.
- [78] K. Suchan, A. Merdasa, C. Rehermann, E. L. Unger, I. G. Schleblykin, *J. Lumin.* **2020**, *221*, 117073.
- [79] J. R. Vicente, J. Chen, *J. Phys. Chem. Lett.* **2020**, *11*, 1802.
- [80] J. R. Vicente, M. E. Kordes, J. Chen, *J. Energy Chem.* **2021**, *63*, 8.
- [81] S. J. Yoon, M. Kuno, P. V. Kamat, *ACS Energy Lett.* **2017**, *2*, 1507.
- [82] A. J. Knight, J. Borchert, R. D. Oliver, J. B. Patel, P. G. Radaelli, H. J. Snaith, M. B. Johnston, L. M. Herz, *ACS Energy Lett.* **2021**, *6*, 799.
- [83] L. A. Frolova, S. Y. Luchkin, Y. Lekina, L. G. Gutsev, S. A. Tsarev, I. S. Zhidkov, E. Z. Kurmaev, Z. X. Shen, K. J. Stevenson, S. M. Aldoshin, P. A. Troshin, *Adv. Energy Mater.* **2021**, *11*, 2002934.
- [84] G. C. Halford, Q. Deng, A. Gomez, T. Green, J. M. Mankoff, R. A. Belisle, *ACS Appl. Mater. Interfaces* **2022**, *14*, 4335.
- [85] V. J. Lim, A. J. Knight, R. D. Oliver, H. J. Snaith, M. B. Johnston, L. M. Herz, *Adv. Funct. Mater.* **2022**, *32*, 2204825.
- [86] W. Rehman, R. L. Milot, G. E. Eperon, C. Wehrenfennig, J. L. Boland, H. J. Snaith, M. B. Johnston, L. M. Herz, *Adv. Mater.* **2015**, *27*, 7938.
- [87] R. E. Beal, N. Z. Hagström, J. Barrier, A. Gold-Parker, R. Prasanna, K. A. Bush, D. Passarello, L. T. Schelhas, K. Brüning, C. J. Tassone, H. G. Steinrück, M. D. McGehee, M. F. Toney, A. F. Nogueira, *Matter* **2020**, *2*, 207.
- [88] D. P. McMeekin, G. Sadoughi, W. Rehman, G. E. Eperon, M. Saliba, M. T. Hörantner, A. Haghighirad, N. Sakai, L. Korte, B. Rech, M. B. Johnston, L. M. Herz, H. J. Snaith, *Science* **2016**, *351*, 151.
- [89] A. Sadhanala, F. Deschler, T. H. Thomas, S. E. Dutton, K. C. Goedel, F. C. Hanusch, M. L. Lai, U. Steiner, T. Bein, P. Docampo, D. Cahen, R. H. Friend, *J. Phys. Chem. Lett.* **2014**, *5*, 2501.
- [90] C. M. Sutter-Fella, Y. Li, M. Amani, J. W. Ager, F. M. Toma, E. Yablonovitch, I. D. Sharp, A. Javey, *Nano Lett.* **2016**, *16*, 800.
- [91] Z. Li, X. Zheng, X. Xiao, Y. An, Y. Wang, Q. Huang, X. Li, R. Checharoen, Q. An, Y. Rong, T. Wang, H. Xu, *Adv. Sci.* **2022**, *9*, 2103948.
- [92] A. D. Wright, C. Verdi, R. L. Milot, G. E. Eperon, M. A. Pérez-Osorio, H. J. Snaith, F. Giustino, M. B. Johnston, L. M. Herz, *Nat. Commun.* **2016**, *7*, 11755.
- [93] W. Mao, C. R. Hall, A. S. Chesman, C. Forsyth, Y.-B. Cheng, N. W. Duffy, T. A. Smith, U. Bach, *Angew. Chem., Int. Ed.* **2019**, *58*, 2893.
- [94] F. Babbe, E. Masquelier, Z. Zheng, C. M. Sutter-Fella, *J. Phys. Chem. C* **2020**, *124*, 24608.
- [95] D. Marongiu, X. Chang, V. Sarritzu, N. Sestu, R. Pau, A. Geddo Lehmann, A. Mattoni, F. Quochi, M. Saba, A. Mura, G. Bongiovanni, *ACS Energy Lett.* **2017**, *2*, 769.
- [96] N. Phung, A. Mattoni, J. A. Smith, D. Skroblin, H. Köbler, L. Choubrac, J. Breternitz, J. Li, T. Unold, S. Schorr, C. Gollwitzer, I. G. Schleblykin, E. L. Unger, M. Saliba, S. Meloni, A. Abate, A. Merdasa, *Joule* **2022**, *6*, 2152.
- [97] A. Pisoni, J. Jačimović, O. S. Barišić, M. Spina, R. Gaál, L. Forró, E. Horváth, *J. Phys. Chem. Lett.* **2014**, *5*, 2488.